

Article

2-Phenyl-4,4,5,5-tetramethylimidazoline-1-oxyl 3-oxide Radical (PTIO●) Trapping Activity and Mechanisms of 16 Phenolic Xanthones

Xican Li ^{1,2,*}, Ban Chen ^{1,2,†}, Xiaojun Zhao ^{1,2} and Dongfeng Chen ^{3,4,*}

¹ School of Chinese Herbal Medicine, Guangzhou University of Chinese Medicine, Waihuan East Road No. 232, Guangzhou Higher Education Mega Center, Guangzhou 510006, China; imchenban@foxmail.com (B.C.); zxj@gzucm.edu.cn (X.Z.)

² Innovative Research & Development Laboratory of TCM, Guangzhou University of Chinese Medicine, Waihuan East Road No. 232, Guangzhou Higher Education Mega Center, Guangzhou 510006, China

³ School of Basic Medical Science, Guangzhou University of Chinese Medicine, Waihuan East Road No. 232, Guangzhou Higher Education Mega Center, Guangzhou 510006, China

⁴ The Research Center of Basic Integrative Medicine, Guangzhou University of Chinese Medicine, Waihuan East Road No. 232, Guangzhou Higher Education Mega Center, Guangzhou 510006, China

* Correspondence: lixc@gzucm.edu.cn or lixican@126.com (X.L.); chen888@gzucm.edu.cn (D.C.); Tel.: +86-203-935-8076 (X.L.)

† These authors contributed equally to this work.

Academic Editor: Susana M. Cardoso

Received: 13 June 2018; Accepted: 10 July 2018; Published: 11 July 2018



Abstract: This study used the 2-phenyl-4,4,5,5-tetramethylimidazoline-1-oxyl 3-oxide radical (PTIO●) trapping model to study the antioxidant activities of 16 natural xanthones in aqueous solution, including garcinone C, γ -mangostin, subelliptenone G, mangiferin, 1,6,7-trihydroxy-xanthone, 1,2,5-trihydroxyxanthone, 1,5,6-trihydroxyxanthone, norathyriol, 1,3,5,6-tetrahydroxy-xanthone, isojacareubin, 1,3,5,8-tetrahydroxyxanthone, isomangiferin, 2-hydroxyxanthone, 7-O-methylmangiferin, neomangiferin, and lancesin. It was observed that most of the 16 xanthones could scavenge the PTIO● radical in a dose-dependent manner at pH 4.5 and 7.4. Among them, 12 xanthones of the *para*-di-OHs (or *ortho*-di-OHs) type always exhibited lower half maximal inhibitory concentration (IC₅₀) values than those not of the *para*-di-OHs (or *ortho*-di-OHs) type. Ultra-performance liquid chromatography coupled with electrospray ionization quadrupole time-of-flight tandem mass spectrometry (UPLC-ESI-Q-TOF-MS/MS) analysis revealed that most of these xanthones gave xanthone-xanthone dimers after incubation with PTIO●, except for neomangiferin. Based on these data, we concluded that the antioxidant activity of phenolic xanthone may be mediated by electron-transfer (ET) plus H⁺-transfer mechanisms. Through these mechanisms, some xanthones can further dimerize unless they bear huge substituents with steric hindrance. Four substituent types (i.e., *para*-di-OHs, 5,6-di-OHs, 6,7-di-OHs, and 7,8-di-OHs) dominate the antioxidant activity of phenolic xanthones, while other substituents (including isoprenyl and 3-hydroxy-3-methylbutyl substituents) play a minor role as long as they do not break the above four types.

Keywords: xanthone; structure-activity relationship; antioxidant; *ortho*-di-OHs; *para*-di-OHs

1. Introduction

Natural xanthones can be isolated from edible plants, medicinal plants (including Chinese herbal medicines [1]), and marine-derived fungi (e.g., *Talaromyces islandicus* EN-501 [2]). Particularly, dozens of xanthones have been successfully isolated from the tropical fruits mangosteen and mango,

and xanthenes have been considered as the bioactive constituents of these fruits [3–6]. Structural elucidation demonstrated that the xanthone scaffold is composed of two phenyl rings and one pyrone ring in the same plane (Figure 1). In this planar and symmetrical scaffold, the hydrogen atom (H) at the 1–8 position can be substituted by -OH to construct phenolic -OHs; thus, xanthenes can be regarded as natural phenolics and serve as phenolic antioxidants [3,4,7].

Phenolic antioxidants were reported to play an important role in disease prevention [5]. For example, mangosteen fruit was recently suggested to have an anti-tumor effect towards hepatic carcinoma [8]. Indeed, anti-tumor activity is closely associated with antioxidant activity. This is because cell carcinogenesis results—to a great extent—from reactive oxygen species (ROS)-induced oxidative damage [9]. Phenolic xanthenes and other phenolics can effectively suppress the excessive ROS to prevent carcinogenesis. Nevertheless, a systematic investigation of the antioxidant activities and mechanisms of the xanthenes family has not yet been reported.

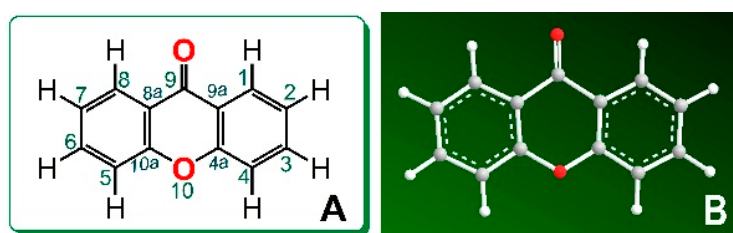


Figure 1. The structure (A) and preferential conformation (B) of the xanthone scaffold.

In the study, a 2-phenyl-4,4,5,5-tetramethylimidazoline-1-oxyl 3-oxide radical (PTIO•, Figure 2) trapping assay was introduced for the investigation. The PTIO•-trapping model has been newly developed by our team [10], and has at least two advantages over the common antioxidant assays, e.g., 1,1-diphenyl-2-picryl-hydrazyl (DPPH•) scavenging assay and 2,2'-azino-bis(3-ethyl-benzothiazoline-6-sulfonic acid) (ABTS•⁺) scavenging assay. Like the •OH radical, the •O₂-anion radical, and other ROS, the PTIO• radical is also an oxygen-centered radical (Figure 2); Like antioxidant action in cells, PTIO• trapping action is also fulfilled in aqueous media; aqueous media however is more biologically relevant [11,12]. Two common antioxidant assays (especially the DPPH•-scavenging assay), however, are based on a nitrogen-centered radical and performed in lipophilic media. Thus, the PTIO•-trapping assay can well characterize the ROS-scavenging action of an antioxidant and is more suitable to study the antioxidant activity of phenolic xanthenes. To research their antioxidant mechanisms, the reaction products of xanthenes with PTIO• were further determined using ultra-performance liquid chromatography coupled with electrospray ionization quadrupole time-of-flight tandem mass spectrometry (UPLC–ESI–Q–TOF–MS/MS) in the study.

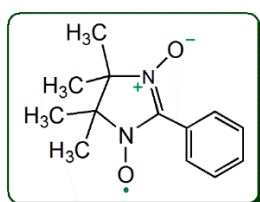


Figure 2. The structure of the 2-phenyl-4,4,5,5-tetramethylimidazoline-1-oxyl 3-oxide radical (PTIO•).

Hypothetically, the antioxidant activities and mechanisms should arise from the effectiveness of some specific substituents in xanthenes. As indicated in the literature [13,14], these substituents mainly refer to phenolic -OH, isoprenyl, cyclized-isoprenyl, methyl, and glycoside. Phenolic -OH, however, can be further classified into several types: *para*-di-OHs, 5,6-di-OHs, 6,7-di-OHs, 7,8-di-OHs, single phenolic -OH, and *meta*-di-OHs. The isoprenyl substituent is considered as a characteristic of

the xanthenes family, because about 50% members contain this substituent [13,14]. Whether and how these substituents affect the antioxidant activities of xanthenes remain unknown until now, despite the fact that at least 300 phenolic xanthenes have already been recorded in the literature [13,14].

To address the above problems, 16 xanthenes were randomly selected as references in this study (Figure 3). As seen in Figure 3, these references covered all the aforementioned substituents. Moreover, they account for about 6% of whole xanthenes [13,14]. Thereby, the study is expected to provide new and characteristic information of phenolic xanthenes.

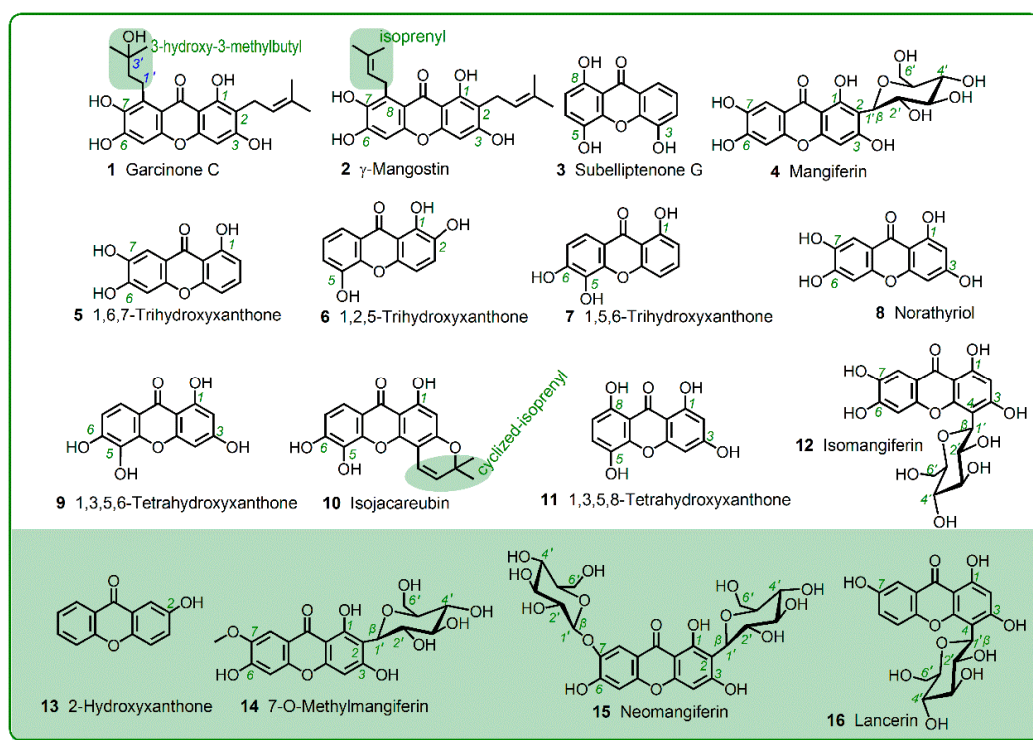


Figure 3. Structures of the 16 selected xanthenes.

2. Results and Discussion

2.1. Antioxidant Activity and Mechanism in PTIO•-Trapping Assay

As suggested by the cyclic voltammogram, PTIO•-trapping below pH 5.0 is an ET process [10]. In the present study, most of xanthenes could scavenge the PTIO• radical in a dose-dependent manner at pH 4.5 (Supplementary Materials S1). This indicated that xanthenes might possess ET potential during the antioxidant process. Furthermore, the PTIO•-trapping activities of these xanthenes were also determined at physiological pH (7.4). PTIO•-trapping action at pH 7.4 may be involved in H⁺-transfer [10]. As shown in Supplementary Materials S1, the PTIO•-trapping percentages of the 16 xanthone references also increased in a concentration-dependent manner at pH 7.4, implying that the antioxidant activity of xanthone may also be involved in H⁺-transfer. In fact, at physiological pH, phenolic -OH with weak acidity may ionize to give rise to H⁺. For example, mangiferin has been demonstrated to be of pK_{a1} 6.52 ± 0.006 (25 °C) [15]. At pH 4.5, its weak acidity may be suppressed by the solution H⁺ ion, thus its H⁺-transfer has been reduced. Accordingly, it exhibited higher IC₅₀ value at pH 4.5, compared with at pH 7.4 (Table 1).

Table 1. The main results of PTIO•-trapping activity of 16 xanthenes using UPLC-ESI-Q-TOF-MS/MS analysis and colorimetric analysis.

No	Xanthone	Main Results of UPLC-ESI-Q-TOF-MS/MS Analysis of Reaction Products				IC ₅₀ in Colorimetric Analysis/μM		Activity
		Retention Time/Min	Primary MS Spectra	MS/MS Spectra	Product	pH 4.5	pH 7.4	
1	Garcinone C	5.961	825, 826, 827	353, 411, 825	dimer	36.0 ± 3.1	40.8 ± 2.0	Strong
2	γ-Mangostin	9.847	789, 790, 791	375, 393, 394, 395, 677	dimer	45.5 ± 2.4	60.4 ± 1.8	
3	Subelliptenone G	1.739	487, 488	No data	dimer	63.4 ± 13.3	110.9 ± 3.8	
4	Mangiferin	1.105	841, 842, 843, 844	329, 419, 601, 631, 661, 721, 751, 823	dimer	64.1 ± 8.5	38.0 ± 2.7	
5	1,6,7-Trihydroxyxanthone	1.813	485, 846, 487	243, 349	dimer	83.0 ± 2.2	90.3 ± 3.0	
6	1,2,5-Trihydroxyxanthone	1.648	487, 488	No data	dimer	89.1 ± 7.4	112.2 ± 0.2	
7	1,5,6-Trihydroxyxanthone	2.044	485, 486, 487, 488	243, 485	dimer	101.3 ± 16.6	116.3 ± 2.2	
8	Norathyriol	1.341	517, 518, 519, 520	229, 257, 258, 259, 365, 499, 517	dimer	103.0 ± 3.7	54.1 ± 0.9	
9	1,3,5,6-Tetrahydroxyxanthone	1.349	517, 518, 519, 520	229, 257, 258, 259, 365, 499, 517	dimer	108.1 ± 19.4	102.7 ± 4.7	
10	Isojacareubin	8.483	649, 650, 651, 652	323-325, 649	dimer	108.7 ± 0.1	136.7 ± 7.3	
11	1,3,5,8-Tetrahydroxyxanthone	1.726	519, 520, 521	215, 259, 260	dimer	116.7 ± 12.6	133.1 ± 29.4	
12	Isomangiferin	1.105	841, 842, 843, 844	329, 419, 601, 631, 661, 721, 751, 823	dimer	121.3 ± 8.3	104.1 ± 12.3	
13	2-Hydroxyxanthone	1.885	423, 424	No data	dimer	284.2 ± 48.8	142.5 ± 13.1	Weak
14	7-O-Methylmangiferin	1.204	871, 872	No data	dimer	387.2 ± 37.5	234.9 ± 1.7	
15	Neomangiferin	No product	No product	No product	No product	545.2 ± 15.2	213.1 ± 23.8	
16	Lancerin	1.165–1.191	811, 812	No data	dimer	681.2 ± 7.9	1106.3 ± 202.6	

The IC₅₀ value was defined as the final concentration of 50% PTIO• radical inhibition and was calculated by linear regression analysis and expressed as the mean ± SD (*n* = 3). The linear regression was analyzed using Origin 6.0 professional software. Trolox is the positive control. Its IC₅₀ values were calculated as 187.5 ± 24.2 μM (pH 4.5) and 175.0 ± 12.4 μM (pH 7.4). The dose-response curves are listed in Supplementary Materials S1; while the original UPLC-ESI-Q-TOF-MS/MS data were listed in Supplementary Materials S18. The 16 xanthenes were classified based on the comparison of IC₅₀ values at pH 4.5. These data were analyzed by independent *t*-test for comparison between two groups. Multiple comparisons within the same group was conducted by one-way ANOVA. *p* < 0.05 was considered statistically significant. The statistical analysis was performed using SPSS 11.5 system (SPSS, Chicago, IL, USA).

To study the antioxidant mechanisms further, each of xanthenes was incubated with the PTIO• radical and the reaction product was subsequently analyzed using UPLC–ESI–Q–TOF–MS/MS. The results in Table 1 revealed that most of these xanthenes gave rise to a dimeric product. For example, after incubation with the PTIO• radical, isojacareubin yielded an isojacareubin-isojacareubin dimer, which displayed a primary MS peak (m/z 649) under negative ion model. This primary MS peak was further observed to cleave to produce m/z 323 and 324 (Table 1 and Supplementary Materials S18). Based on these MS spectral data and previous work [16], the dimerization reaction of isojacareubin can be proposed as Figure 4A; while the MS spectra elucidation is described in Figure 4B.

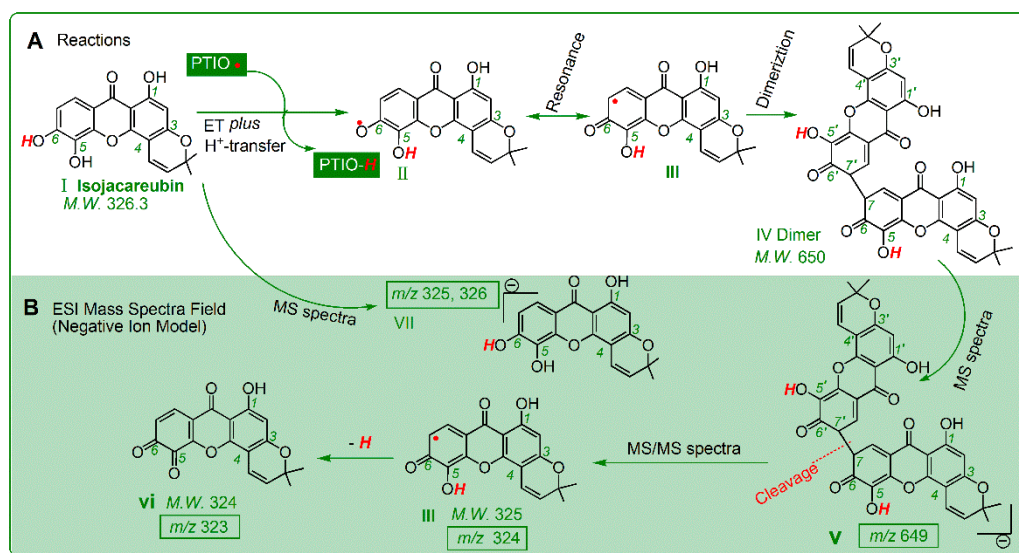


Figure 4. The possible reactions of isojacareubin with PTIO• (A), and the MS spectra elucidations (B) (The m/z value is expressed as an integer; precise m/z values are detailed in Supplementary Materials S18.).

In the proposed reactions (Figure 4), the covalent bond between the 7- and 7'- positions has linked two isojacareubin radicals (III), to generate one isojacareubin-isojacareubin dimer (IV). The generation of a dimer can be considered as the consequence of ET *plus* H⁺-transfer (Figure 4). If there is no H⁺-transfer, there will be no peak of m/z 649 in the product. On the other hand, if there is only H⁺-transfer and no ET, there will be a phenoxy anion; two phenoxy anions however cannot combine with each other via covalency. Therefore, the evidence from UPLC–ESI–Q–TOF–MS/MS analysis can further verify the occurrence of ET *plus* H⁺-transfer.

It is worth mentioning that, (i) the dimerization reaction may be more complicated than that in Figure 4, and the covalent bond can also be linked to other positions [17–19]. Nevertheless, it is doubtless that the dimeric isojacareubin-isojacareubin is formed. (ii) The only xanthone that did not give a dimer product was neomangiferin (Table 1) bearing two sugar residues. This can be attributed to the fact that the two sugar residues have huge substituents and may hinder the radical adduct formation (RAF) potential. The RAF product however was supported by the earlier literatures where it was termed as nonradical product [11,20,21].

2.2. Antioxidant Role of Phenolic -OH: Evidence From PTIO•-Trapping Assay

Results from the colorimetric method revealed that there was a great difference in the H⁺-transfer (or ET) potentials among the 16 references (Table 1). At pH 4.5, the values of IC₅₀ varied from 36.0 μM to 681.2 μM. Particularly, there was an evident gap in IC₅₀ values at pH 4.5 between the former twelve xanthenes (1–12, IC₅₀ = 36.0–121.3 μM, pH = 4.5) and the latter four xanthenes (13–16, IC₅₀ = 284.2–681.2 μM, pH = 4.5, Table 1). The latter four xanthenes contained neither *para*-di-OHs nor *ortho*-di-OHs. In this case, even with multiple phenolic -OHs, the xanthone still exhibited very low high

IC₅₀ values, e.g., neomangiferin (15). The data of neomangiferin clearly indicated that, *para*-di-OHs (or *ortho*-di-OHs) played a critical role in antioxidant activity at pH 4.5; and single phenolic -OHs and *meta*-di-OHs type played a negligible role. As seen in Table 1, both *para*-di-OHs and *ortho*-di-OHs xanthenes are classified into the strong group based on the IC₅₀ values at pH 4.5, implying that the role of *para*-di-OHs is roughly equivalent to that of *ortho*-di-OHs. A typical example was the pair of 9 vs. 11 at pH 4.5; A similar situation was also observed at pH 7.4. At pH 7.4, however, the PTIO•-trapping has been mentioned to be mediated by H⁺-transfer [10]. Thus, it can be inferred that *para*-di-OHs or *ortho*-di-OHs may similarly govern the ET *plus* H⁺-transfer potentials.

Further analysis suggested that *ortho*-di-OHs could be divided into 3 types, i.e., 5,6-di-OHs (e.g., 7, 9, and 10), 6,7-di-OHs (e.g., 1, 2, 4, 5, 8, and 12), and 7,8-di-OHs (e.g., 6). The fact that the IC₅₀ values of 3 xanthenes (1,6,7-trihydroxyxanthone (5), 1,2,5-trihydroxyxanthone (6), and 1,5,6-trihydroxyxanthone (7)) are not significantly different ($p > 0.05$) at pH 4.5 suggests that the *ortho*-di-OHs positions (5,6-position, 6,7- position, or 7,8-position) have not affected the antioxidant activity. This suggestion can partly explain the similarities of a pair of xanthenes: norathyriol (8) and its isomer 1,3,5,6-tetrahydroxyxanthone (9). As shown in Table 1, in PTIO•-trapping colorimetric analysis, there is no significant difference ($p > 0.05$) in IC₅₀ values at pH 4.5 between them. In PTIO•-trapping UPLC–ESI–Q–TOF–MS/MS analysis, norathyriol and its isomer produced a similar series of MS peaks (Table 1 and Supplementary Materials S18). Based on the MS spectra elucidation, it is presumed that these two isomers have undergone similar dimerization reactions (Supplementary Materials S19,20).

In short, during the PTIO•-trapping process, *meta*-di-OHs have a negligible effect on the occurrence of ET *plus* H⁺-transfer reactions, and each of the other four substituent types (*para*-di-OHs, 5,6-di-OHs, 6,7-di-OHs, and 7,8-di-OHs) can govern the antioxidant activity of phenolic xanthenes. However, if any of the four types is broken, the antioxidant activity is remarkably decreased. For example, when 6,7-di-OHs in mangiferin (4) were broken by a glucoside to form neomangiferin (15), the IC₅₀ values were greatly increased (8.5-times for pH 4.5 and 5.6-times for pH 7.5, Table 1).

Our findings regarding the role of *ortho*-di-OHs was further supported by a number of reports, which usually referred to *ortho*-di-OHs as the catechol moiety [22–26]. The reason why the *ortho*-di-OHs play a critical role in antioxidant xanthenes may be the fact that *ortho*-di-OHs can be oxidized to *ortho*-benzo quinone by free radicals [27,28]. For example, in the reaction of isojacareubin with PTIO•, 5,6-di-OHs is oxidized to 5,6-*ortho*-benzoquinone via ET *plus* H⁺-transfer mechanisms [29,30] (Figure 4). Similarly, *para*-di-OHs type could be hypothesized to transform into *para*-benzoquinone, in accordance with Figure 4. In fact, the *para*-di-OHs molecule itself has strong antioxidant activity. It is now clear that the stability of *para*-benzoquinone or *ortho*-benzoquinone can be responsible for the strong antioxidant activity of *para*-di-OHs (or *ortho*-di-OHs) type. Our experimental data and deduction denied the opinion of a minor role of *ortho*-di-OHs type (catechol moiety) [31].

It must be emphasized that (1) the antioxidant role of *para*-di-OHs type in natural phenolics has not been mentioned previously [32]. This may be attributed to the fact that *para*-di-OHs are hardly found in flavonoids [13,14,26,33] and other phenolics [13,14,19,22–31,34,35]. For instance, among thousands of flavonoids, only 5 *para*-di-OHs flavonoids (i.e., 5,8-dihydroxy-flavonoids) have been documented: rhodionin [36], 5,8-dihydroxy-3,6,7-trimethoxyflavone [37], 5,8-dihydroxy-6,7-dimethoxyflavone [37], 5,8-dihydroxy-6,7,4'-trimethoxyflavone, and 5,8-dihydroxy-6,7,3',4',5'-pentamethoxyflavone [38]. Thereby, our findings may be of great scientific value. (2) ET *plus* H⁺-transfer reactions can cover several possible mechanisms, such as hydrogen atom transfer (HAT), sequential proton-loss electron-transfer (SPLET), electron transfer–proton transfer (ET–PT), and proton coupled electron transfer (PCET) [35,39]. Because these antioxidant mechanisms are essentially involved in ET and H⁺-transfer reactions. The difference among these mechanisms depends on the sequence and cooperativity [40]. Thus, the net result of all these different antioxidant mechanisms is identical; and the proposed reactions in Figure 4 are basically acceptable. Our proposal is also supported by the recent report concerning phenolic antioxidant reaction with alkylperoxyl radical (ROO•) [41].

2.3. Antioxidant Role of Other Substituents: Evidence from the PTIO•-Trapping Assay

As discussed above, other substituents may also affect the antioxidant activity of xanthenes. These substituents include isoprenyl, cyclized-isoprenyl, methyl, and glycoside. The isoprenyl substituent frequently appears in xanthenes, and seldom occurs in other phenolics (such as flavonoid, lignanoid, coumarin, and stilbene [13,14,23,25,42–46]). As a result, its role has not been analyzed by means of the structure-activity relationship [40]. In the study, γ -mangostin (**2**), an isoprenylated xanthone was found to be superior to its parent compound norathyriol (**8**) at pH 4.5.

This suggested that the isoprenyl substituent enhances the ET potential. Possibly through hydrolysis, isoprenyl substituent can also be transferred into 3-hydroxy-3-methylbutyl substituent. Thus, 3-hydroxy-3-methylbutyl substituent can also be found in xanthenes (e.g., **1**, Figure 3). As shown in Table 1, there was no great difference between garcinone C (**1**) and γ -mangostin (**2**); Thus, the effect of the 3-hydroxy-3-methylbutyl substituent was basically equivalent to that of the isoprenyl substituent. In addition, the cyclized-isoprenyl substituent was also found in xanthone (e.g., **10**, Figure 3). Comparison of the IC₅₀ values of 1,3,5,6-tetrahydroxyxanthone (**9**) and isojacareubin (**10**) revealed that the cyclized-isoprenyl substituent decreases the antioxidant activity (Table 1). This may be attributed to the fact that the cyclized-isoprenyl substituent replaces a phenolic -OH at the 3-position.

Like the cyclized-isoprenyl substituent, the methyl substituent may also replace phenolic -OHs. A typical example was mangiferin (**4**) and its ether 7-O-methylmangiferin (**14**). As shown in Table 1, the IC₅₀ values at two pH values (pH 4.5 and 7.4) decrease significantly from mangiferin (**4**) to 7-O-methylmangiferin (**14**). This is because methylation breaks the 6,7-di-OHs construction in mangiferin (**4**).

Like the methyl substituent, the glycoside substituent frequently occurs in phenolic antioxidants (including xanthenes). As seen in Table 1, both mangiferin (**4**) and isomangiferin (**12**) can be regarded as the glycosidated derivatives of norathyriol (**8**); and mangiferin (**4**) and isomangiferin (**12**) are actually two positional-isomers of each other. However, in the study, the three xanthenes were classified into as the strong antioxidants (Table 1). The fact implies that, the effect of glycoside substituent at any C-position is very limited.

In brief, during the PTIO•-trapping process, the above substituents played a minor role in antioxidant activity. However, when these substituents break the aforementioned four types (*para*-di-OHs, 5,6-di-OHs, 6,7-di-OHs, and 7,8-di-OHs), they can greatly lower the antioxidant activity of xanthenes.

3. Materials and Methods

3.1. Chemicals and Animals

2-Phenyl-4,4,5,5-tetramethylimidazoline-1-oxyl 3-oxide radical (PTIO•, CAS 18390-00-6, >98.0%, M.W. 233.29) was purchased from TCI Chemical Co. (Shanghai, China). (\pm)-6-Hydroxyl-2,5,7,8-tetramethylchromane-2-carboxylic acid (Trolox, CAS 53188-07-1, 97%, M.W. 250.29) was purchased from Sigma-Aldrich Shanghai Trading Co. (Shanghai, China). Garcinone C (CAS 76996-27-5, C₂₃H₂₆O₇, M.W. 414.5, 98%, Supplementary Materials S2) and γ -mangostin (CAS 31271-07-5, C₂₃H₂₄O₆, M.W. 396.4, 97%, Supplementary Materials S3) were purchased from Chengdu Biopurify Phytochemicals Ltd. (Chengdu, China). Subelliptenone G (CAS 162473-22-5, C₁₃H₈O₅, M.W. 244.2, purity 97%, Supplementary Materials S4) was purchased from BioBioPha Co., Ltd. (Kunming, China). Mangiferin (CAS 4773-96-0, C₁₉H₁₈O₁₁, M.W. 422.3, 98%, Supplementary Materials S5) was purchased from Chengdu Biopurify Phytochemicals Ltd. 1,6,7-Trihydroxyxanthone (CAS 25577-04-2, C₁₃H₈O₅, M.W. 244.2, purity 98%, Supplementary Materials S6), 1,2,5-trihydroxyxanthone (CAS 156640-23-2, C₁₃H₈O₅, M.W. 244.2, purity 98%, Supplementary Materials S7), 1,5,6-trihydroxyxanthone (CAS 5042-03-5, C₁₃H₈O₅, M.W. 244.2, purity 98%, Supplementary Materials S8), norathyriol (CAS 3542-72-1, C₁₃H₈O₆, M.W. 260.2, purity 98%, Supplementary Materials S9), 1,3,5,6-tetrahydroxyxanthone (CAS 5084-31-1, C₁₃H₈O₆, M.W. 260.2, purity 98%, Supplementary Materials S10) and isojacareubin (CAS 50597-93-8, C₁₈H₁₄O₆, M.W. 326.3, purity 97%,

Supplementary Materials S11) were purchased from BioBioPha Co., Ltd. 1,3,5,8-Tetrahydroxyxanthone (CAS 2980-32-7, C₁₃H₈O₆, M.W. 260.2, 98%, Supplementary Materials S12), and isomangiferin (CAS 24699-16-9, C₁₉H₁₈O₁₁, M.W. 422.3, 98%, Supplementary Materials S13) were purchased from Chengdu Biopurify Phytochemicals Ltd. 2-Hydroxyxanthone (CAS 1915-98-6, C₁₃H₈O₃, M.W. 212.2, purity 98%, Supplementary Materials S14) was purchased from BioBioPha Co., Ltd. 7-O-Methylmangiferin (CAS 31002-12-7, C₂₀H₂₀O₁₁, M.W. 436.1, purity 97%, Supplementary Materials S15), neomangiferin (CAS 64809-67-2, C₂₅H₂₈O₁₆, M.W. 584.5, purity 97%, Supplementary Materials S16) and lincerin (CAS 81991-99-3, C₁₉H₁₈O₁₀, M.W. 406.3, purity 98%, Supplementary Materials S17) were purchased from Chengdu Biopurify Phytochemicals Ltd. Other reagents were of analytical grade.

3.2. PTIO•-Trapping Colorimetric Assay

The PTIO•-trapping assay was conducted based on our previously published method [10]. The experimental procedures are briefly described as following: PTIO• radical was dissolved in phosphate pH 4.5 and pH 7.4 buffer to prepare PTIO• solution; xanthone samples were prepared using methanol. Various volumes of xanthone methanolic were brought to phosphate pH 4.5 and pH 7.4 buffer, then were mixed with PTIO• solution. After incubation for 12 h, the product mixture were measured at 560 nm on a microplate reader (Multiskan FC, Thermo Scientific, Shanghai, China). The PTIO• inhibition percentage was calculated as follows:

$$\text{Inhibition \%} = \frac{A_0 - A}{A_0} \times 100\% \quad (1)$$

where A_0 is the absorbance at 560 nm of the control without the sample, and A is the absorbance at 560 nm of the reaction mixture with the sample. The above experiment was repeated using phosphate buffers with different pH values (including pH 4.5 and 7.4).

3.3. UPLC–ESI–Q–TOF–MS/MS Analysis of Xanthone Reaction Product with PTIO•

UPLC–ESI–Q–TOF–MS/MS spectra of the reaction products of PTIO• with the xanthone were obtained according to our previously described method [47]. The methanolic solutions of phenolic components were mixed with a solution of PTIO• radicals in methanol at a molar ratio of 1:2, and the resulting mixtures were incubated for 24 h at room temperature. The product mixtures were filtered through a 0.22- μ m filter and measured using a UPLC–ESI–Q–TOF–MS/MS system equipped with a C₁₈ column (2.0 mm i.d. \times 100 mm, 2.2 μ m, Shimadzu Co., Kyoto, Japan). The mobile phase was used for elution and consisted of a mixture of methanol (phase A) and water (phase B). The column was eluted at a flow rate of 0.3 mL/min with the following gradient elution program: 0–10 min, 60–100% A; 10–15 min, 100% A. The sample injection volume was set at 1 μ L to separate the components, and the column temperature was 40 °C. The Q–TOF–MS/MS analysis was conducted on a Triple TOF 5600+ mass spectrometer (AB SCIEX, Framingham, MA, USA) equipped with an ESI source, which was run in the negative ionization mode. The scan range was set at 50–1600 Da. The system was run with the following parameters: ion spray voltage, –4500 V; ion source heater, 550 °C; curtain gas (CUR, N₂), 30 psi; nebulizing gas (GS1, air), 50 psi; and TurboIonSpray (TIS) gas (GS2, air), 50 psi. The declustering potential (DP) was set at –100 V, and the collision energy (CE) was set at –40 V with a collision energy spread (CES) of 20 V. The RAF products were quantified by the extracting the corresponding formula (e.g., [C₂₆H₁₄O₁₂–H][–] for the norathyriol–norathyriol dimer) from the total ion chromatogram and integrating the corresponding peaks [48,49].

3.4. Statistical Analysis

Each experiment was performed in triplicate and the data were recorded as mean \pm SD (standard deviation). The dose–response curves were plotted using Origin 6.0 professional software (OriginLab, Northampton, MA, USA). The IC₅₀ value was defined as the final concentration of 50% radical inhibition (or relative reducing power) [50]. It was calculated by linear regression analysis,

and expressed as the mean \pm SD ($n = 3$). The linear regression was analyzed using Origin 6.0. Determination of significant differences between the mean IC₅₀ values was performed using one-way ANOVA and the *t*-test. The analysis was performed using SPSS software 13.0 for Windows (SPSS Inc., Chicago, IL, USA). $p < 0.05$ was considered to be statistically significant.

4. Conclusions

Phenolic xanthenes may react via ET plus H⁺-transfer to present antioxidant activity. Through these mechanisms, most xanthenes can further dimerize unless they bear huge substituents with steric hindrance. The antioxidant activity of phenolic xanthenes is governed by any of four substituent types, i.e., *para*-di-OHs, 5,6-di-OHs, 6,7-di-OHs, and 7,8-di-OHs. The effects of other types of substituents are very limited. In general, isoprenyl and 3-hydroxy-3-methylbutyl substituents can slightly enhance ET potential. Cyclized-isoprenyl, methyl, and glycoside substituents can cut down phenolic -OH to lower antioxidant activity. However, if these substituents break the aforementioned four types, their detrimental effect may be enhanced.

Supplementary Materials: The following are available online. Supplementary Materials S1 Dose response curves and IC₅₀ values; Supplementary Materials S2–17 Analysis certificates and appearances of 16 xanthenes. Supplementary Materials S18 Original MS spectra; Supplementary Materials S19 dimerization reaction of norathyriol and MS spectra elucidation; Supplementary Materials S20 dimerization reaction of 1,3,5,6-tetrahydroxyxanthone and MS spectra elucidation.

Author Contributions: X.L. conceived and D.C. designed the experiments; B.C. conducted the experiments; X.L. wrote the paper. All authors read and approved the final manuscript.

Funding: This work was supported by Guangdong Provincial Education Office Science and Technology Project (2017KCXTD007), National Nature Science Foundation of China (81573558), Guangdong Science and Technology Project (2017A050506043), and Natural Science Foundation of Guangdong Province (2017A030312009).

Acknowledgments: None.

Conflicts of Interest: The authors declare that they have no competing interests.

Abbreviations

The following abbreviations are used in this manuscript:

ABTS● ⁺	2,2'-azino-bis(3-ethylbenzothiazoline-6-sulphonic acid)
DPPH●	1,1-diphenyl-2-picryl-hydrazyl radical
ET	electron transfer
ET-PT	electron transfer–proton transfer
HAT	hydrogen atom transfer
PCET	proton coupled electron transfer
PTIO●	2-phenyl-4,4,5,5-tetramethylimidazoline-1-oxyl 3-oxide radical
RAF	radical adduct formation
ROS	reactive oxygen species
SD	standard deviation
SPLET	sequential proton-loss electron-transfer
Trolox	(±)-6-hydroxy-2,5,7,8-tetramethylchromane-2-carboxylic acid
UPLC–ESI–Q–TOF–MS/MS	ultra-performance liquid chromatography coupled with electrospray ionization quadrupole time-of-flight tandem mass spectrometry

References

- Han, Q.B.; Yang, L.; Wang, Y.L.; Qiao, C.F.; Song, J.Z.; Sun, H.D.; Xu, H.X. A pair of novel cytotoxic polyprenylated xanthone epimers from gamboges. *Chem. Biodivers.* **2006**, *3*, 101–105. [[CrossRef](#)] [[PubMed](#)]
- Li, H.L.; Li, X.M.; Liu, H.; Meng, L.H.; Wang, B.G. Two New Diphenylketones and a New Xanthone from *Talaromyces islandicus* EN-501, an Endophytic Fungus Derived from the Marine Red Alga *Laurencia okamurai*. *Mar. Drugs* **2016**, *14*, 223. [[CrossRef](#)] [[PubMed](#)]

3. Yang, R.; Li, P.; Li, N.; Zhang, Q.; Bai, X.; Wang, L.; Xiao, Y.; Sun, L.; Yang, Q.; Yan, J. Xanthonenes from the Pericarp of *Garcinia mangostana*. *Molecules* **2017**, *22*, 683. [[CrossRef](#)] [[PubMed](#)]
4. Jung, H.A.; Su, B.N.; Keller, W.J.; Mehta, R.G.; Kinghorn, A.D. Antioxidant xanthonenes from the pericarp of *Garcinia mangostana* (Mangosteen). *J. Agric. Food Chem.* **2006**, *54*, 2077–2082. [[CrossRef](#)] [[PubMed](#)]
5. Ramirez, J.E.; Zambrano, R.; Sepúlveda, B.; Simirgiotis, M.J. Antioxidant Properties and HPLC-MS Profiling of Chilean Pica Mango Fruits (*Mangifera indica* L. Cv. piqueño). *Molecules* **2014**, *19*, 438–458. [[CrossRef](#)] [[PubMed](#)]
6. Schieber, A.; Berardini, N.; Carle, R. Identification of flavonol and xanthone glycosides from mango (*Mangifera indica* L. Cv. Tommy Atkins) peels by high-performance liquid chromatography-electrospray ionization mass spectrometry. *J. Agric. Food Chem.* **2003**, *51*, 5006–5011. [[CrossRef](#)] [[PubMed](#)]
7. Panda, S.S.; Chand, M.; Sakhuja, R.; Jain, S.C. Xanthonenes as Potential Antioxidants. *Cur. Med. Chem.* **2013**, *20*, 4481–4507. [[CrossRef](#)]
8. Priya, V.; Jainu, M.; Mohan, S. Biochemical Evidence for the Antitumor Potential of *Garcinia mangostana* Linn. On Diethylnitrosamine-Induced Hepatic Carcinoma. *Pharmacogn. Mag.* **2018**, *14*, 186–190. [[PubMed](#)]
9. Kryston, T.B.; Georgiev, A.B.; Pissis, P.; Georgakilas, A.G. Role of oxidative stress and DNA damage in human carcinogenesis. *Mutat. Res.* **2011**, *711*, 193–201. [[CrossRef](#)] [[PubMed](#)]
10. Li, X. 2-Phenyl-4,4,5,5-tetramethylimidazoline-1-oxyl 3-Oxide (PTIO•) Radical Scavenging: A New and Simple Antioxidant Assay *In Vitro*. *J. Agric. Food Chem.* **2017**, *65*, 6288–6297. [[CrossRef](#)] [[PubMed](#)]
11. Amorati, R.; Valgimigli, L. Methods to Measure the Antioxidant Activity of Phytochemicals and Plant Extracts. *J. Agric. Food Chem.* **2018**, *66*, 3324–3329. [[CrossRef](#)] [[PubMed](#)]
12. Litwinienko, G.; Ingold, K.U. Solvent Effects on the Rates and Mechanisms of Reaction of Phenols with Free Radicals. *Acc. Chem. Res.* **2007**, *40*, 222–230. [[CrossRef](#)] [[PubMed](#)]
13. Qin, H.L.; Yu, D.Q. *¹H-NMR Spectroscopic Databook of Natural Products*, 1st ed.; Chemical Industry Press: Beijing, China, 2011; pp. 881–2235.
14. Yang, J.S. *¹³C-NMR Spectroscopic Databook of Natural Products*; Chemical Industry Press: Beijing, China, 2011; pp. 1630–2285.
15. Gómez-Zaleta, B.; Ramírez-Silva, M.T.; Gutiérrez, A.; González-Vergara, E.; Güizado-Rodríguez, M.; Rojas-Hernández, A. UV/vis, ¹H, and ¹³C NMR spectroscopic studies to determine mangiferin pKa values. *Spectrochim. Acta A Mol. Biomol. Spectrosc.* **2006**, *64*, 1002–1009. [[CrossRef](#)] [[PubMed](#)]
16. Bondet, V.; Brand-Williams, W.; Berset, C. Kinetics and mechanisms of antioxidant activity using the DPPH free radical method. *LWT-Food Sci. Technol.* **1997**, *30*, 609–615. [[CrossRef](#)]
17. Krishnamachari, V.; Levine, L.H.; Zhou, C.; Pare, P.W. In vitro flavon-3-ol oxidation mediated by a B ring hydroxylation pattern. *Chem. Res. Toxicol.* **2004**, *17*, 795–804. [[CrossRef](#)] [[PubMed](#)]
18. Fourre, I.; Di Meo, F.; Podlouchka, P.; Otyepka, M.; Trouillas, P. Dimerization of quercetin, Diels-Alder vs. radical-coupling approach: A joint thermodynamics, kinetics, and topological study. *J. Mol. Model.* **2016**, *22*, 190. [[CrossRef](#)] [[PubMed](#)]
19. Krishnamachari, V.; Levine, L.H.; Pare, P.W. Flavonoid oxidation by the radical generator AIBN: A unified mechanism for quercetin radical scavenging. *J. Agric. Food Chem.* **2002**, *50*, 4357–4363. [[CrossRef](#)] [[PubMed](#)]
20. Burton, G.W.; Doba, T.; Gabe, E.; Ingold, K.U. Autoxidation of biological molecules. 4. Maximizing the antioxidant activity of phenols. *J. Am. Chem. Soc.* **1985**, *107*, 7053–7065. [[CrossRef](#)]
21. Lucarini, M.; Pedulli, G.F. Free radical intermediates in the inhibition of the autoxidation reaction. *Chem. Soc. Rev.* **2010**, *39*, 2106–2119. [[CrossRef](#)] [[PubMed](#)]
22. Heim, K.E.; Tagliaferro, A.R.; Bobilya, D.J. Flavonoid antioxidants: Chemistry, metabolism and structure-activity relationships. *J. Nutr. Biochem.* **2002**, *13*, 572–584. [[CrossRef](#)]
23. Li, X.; Li, K.; Xie, H.; Xie, Y.; Li, Y.; Zhao, X.; Jiang, X.; Chen, D. Antioxidant and Cytoprotective Effects of the Di-O-Caffeoylquinic Acid Family: The Mechanism, Structure-Activity Relationship, and Conformational Effect. *Molecules* **2018**, *23*, 222. [[CrossRef](#)] [[PubMed](#)]
24. De La Cruz, J.P.; Ruiz-Moreno, M.I.; Guerrero, A.; Lopez-Villodres, J.A.; Reyes, J.J.; Espartero, J.L.; Labajos, M.T.; Gonzalez-Correa, J.A. Role of the catechol group in the antioxidant and neuroprotective effects of virgin olive oil components in rat brain. *J. Nutr. Biochem.* **2015**, *26*, 549–555. [[CrossRef](#)] [[PubMed](#)]
25. Li, X.; Wu, X.; Huang, L. Correlation between antioxidant activities and phenolic contents of radix angelicae sinensis (danggui). *Molecules* **2009**, *14*, 5349–5361. [[CrossRef](#)] [[PubMed](#)]

26. Liu, J.; Li, X.; Lin, J.; Li, Y.; Wang, T.; Jiang, Q.; Chen, D. *Sarcandra glabra* (*Caoshanhu*) protects mesenchymal stem cells from oxidative stress: A bioevaluation and mechanistic chemistry. *BMC Complement. Altern. Med.* **2016**, *16*, 423. [[CrossRef](#)] [[PubMed](#)]
27. Li, X.; Xie, Y.; Xie, H.; Yang, J.; Chen, D. π - π Conjugation Enhances Oligostilbene's Antioxidant Capacity: Evidence from α -Viniferin and Caraphenol A. *Molecules* **2018**, *23*, 694. [[CrossRef](#)] [[PubMed](#)]
28. Ali, H.M.; Ali, I.H. Energetic and electronic computation of the two-hydrogen atom donation process in catecholic and non-catecholic anthocyanidins. *Food Chem.* **2018**, *243*, 145–150. [[CrossRef](#)] [[PubMed](#)]
29. Yamaguchi, L.F.; Lago, J.H.; Tanizaki, T.M.; Mascio, P.D.; Kato, M.J. Antioxidant activity of prenylated hydroquinone and benzoic acid derivatives from *Piper crassinervium* Kunth. *Phytochemistry* **2006**, *67*, 1838–1843. [[CrossRef](#)] [[PubMed](#)]
30. Dong, L.M.; Jia, X.C.; Luo, Q.W.; Zhang, Q.; Luo, B.; Liu, W.B.; Zhang, X.; Xu, Q.L.; Tan, J.W. Phenolics from *Mikania micrantha* and Their Antioxidant Activity. *Molecules* **2017**, *22*, 1140. [[CrossRef](#)] [[PubMed](#)]
31. Woodman, O.; Meeker, W.; Boujaoude, M. Vasorelaxant and antioxidant activity of flavonols and flavones: Structure-activity relationships. *J. Cardiovasc. Pharm.* **2005**, *46*, 302–309. [[CrossRef](#)]
32. Valgimigli, L.; Amorati, R.; Fumo, M.G.; Dilabio, G.A.; Pedulli, G.F.; Ingold, K.U.; Pratt, D.A. The unusual reaction of semiquinone radicals with molecular oxygen. *J. Org. Chem.* **2008**, *73*, 1830–1841. [[CrossRef](#)] [[PubMed](#)]
33. Li, X.; Wang, L.; Han, W.; Mai, W.; Han, L.; Chen, D. Amentoflavone protects against hydroxyl radical-induced DNA damage via antioxidant mechanism. *Turk. J. Biochem.* **2014**, *39*, 30–36. [[CrossRef](#)]
34. Wang, T.T.; Li, X.C.; Li, Y.R.; Chen, D.F. Mechanistic chemistry of extraordinary capacity of salvianolic acid B on oxidatively damaged mesenchymal stem cells. *J. Chin. Chem. Soc.* **2016**, *63*, 924–929. [[CrossRef](#)]
35. Apak, R.; Ozyurek, M.; Guclu, K.; Capanoglu, E. Antioxidant Activity/Capacity Measurement. 1. Classification, Physicochemical Principles, Mechanisms, and Electron Transfer (ET)-Based Assays. *J. Agric. Food Chem.* **2016**, *64*, 997–1027. [[CrossRef](#)] [[PubMed](#)]
36. Li, T.; Zhang, H. Identification and comparative determination of rhodioidin in traditional tibetan medicinal plants of fourteen *Rhodiola* species by high-performance liquid chromatography-photodiode array detection and electrospray ionization-mass spectrometry. *Chem. Pharm. Bull. (Tokyo)* **2008**, *56*, 807–814. [[CrossRef](#)] [[PubMed](#)]
37. Guerreiro, E.; Kavka, J.; Giordano, O.S. 5,8-Dihydroxy-3,6,7-trimethoxyflavone from *Gnaphalium gaudichaudianum*. *Phytochemistry* **1982**, *21*, 2601–2603. [[CrossRef](#)]
38. Briante, R.; Ferdinando Febbraio, A.; Nucci, R. Antioxidant Properties of Low Molecular Weight Phenols Present in the Mediterranean Diet. *J. Agric. Food Chem.* **2003**, *51*, 6975–6981. [[CrossRef](#)] [[PubMed](#)]
39. Markovic, S.; Tosovic, J. Comparative study of the antioxidative activities of caffeoylquinic and caffeic acids. *Food Chem.* **2016**, *210*, 585–592. [[CrossRef](#)] [[PubMed](#)]
40. Zhang, H.; Wu, W.; Mo, Y. Study of proton-coupled electron transfer (PCET) with four explicit diabatic states at the ab initio level. *Comput. Theor. Chem.* **2017**, *1116*, 50–58. [[CrossRef](#)]
41. Amorati, R.; Baschieri, A.; Morroni, G.; Gambino, R.; Valgimigli, L. Peroxyl Radical Reactions in Water Solution: A Gym for Proton-Coupled Electron-Transfer Theories. *Chem. Eur. J.* **2016**, *22*, 7924–7934. [[CrossRef](#)] [[PubMed](#)]
42. Chen, D.; Li, X.; Xu, Z.; Liu, X.; Du, S.; Li, H.; Zhou, J.; Zeng, H.; Hua, Z. Hexadecanoic Acid from Buzhong Yiqi Decoction Induced Proliferation of Bone Marrow Mesenchymal Stem Cells. *J. Med. Food* **2010**, *13*, 967–975. [[CrossRef](#)] [[PubMed](#)]
43. Li, X.; Hu, Q.; Jiang, S.; Li, F.; Lin, J.; Han, L.; Hong, Y.; Lu, W.; Gao, Y.; Chen, D. Flos *Chrysanthemi Indici* protects against hydroxyl-induced damages to DNA and MSCs via antioxidant mechanism. *J. Saudi. Chem. Soc.* **2015**, *19*, 454–460. [[CrossRef](#)]
44. Lin, J.; Li, X.; Chen, L.; Lu, W.; Chen, X.; Han, L.; Chen, D. Protective effect against hydroxyl radical-induced DNA damage and antioxidant mechanism of [6]-gingerol: A Chemical Study. *Bull. Korean Chem. Soc.* **2014**, *35*, 1633–1638. [[CrossRef](#)]
45. Li, X.; Han, L.; Li, Y.; Zhang, J.; Chen, J.; Lu, W.; Zhao, X.; Lai, Y.; Chen, D.; Wei, G. Protective Effect of Sinapine against Hydroxyl Radical-Induced Damage to Mesenchymal Stem Cells and Possible Mechanisms. *Chem. Pharm. Bull. (Tokyo)* **2016**, *64*, 319–325. [[CrossRef](#)] [[PubMed](#)]

46. Li, X.; Liu, J.; Zhao, Z.; Wang, T.; Lin, J.; Chen, D. Effects of Natural Chalcone-Tannin Hybrids Protecting Mesenchymal Stem Cells against ROS-mediated Oxidative Damage and Indexes for Antioxidant Mechanisms. *Chem. Lett.* **2016**, *45*, 743–745. [[CrossRef](#)]
47. Marin, M.; Manez, S. Recent trends in the pharmacological activity of isoprenyl phenolics. *Curr. Med. Chem.* **2013**, *20*, 272–279. [[CrossRef](#)] [[PubMed](#)]
48. Xie, H.; Li, X.; Ren, Z.; Qiu, W.; Chen, J.; Jiang, Q.; Chen, B.; Chen, D. Antioxidant and cytoprotective effects of Tibetan tea and its phenolic components. *Molecules* **2018**, *23*, 179. [[CrossRef](#)] [[PubMed](#)]
49. Li, X.; Xie, Y.; Li, K.; Wu, A.; Xie, H.; Guo, Q.; Xue, P.; Maleshibek, Y.; Zhao, W.; Guo, J.; et al. Antioxidation and Cytoprotection of Acteoside and Its Derivatives: Comparison and Mechanistic Chemistry. *Molecules* **2018**, *23*, 498. [[CrossRef](#)] [[PubMed](#)]
50. Jiang, Q.; Li, X.C.; Tian, Y.G.; Lin, Q.Q.; Xie, H.; Lu, W.B.; Chi, Y.G.; Chen, D.F. Lyophilized Aqueous Extracts of *Mori Fructus* and *Mori Ramulus* Protect Mesenchymal Stem Cells from •OH-Treated Damage: Bioassay and Antioxidant Mechanism. *BMC Complement. Altern. Med.* **2017**, *17*, 242. [[CrossRef](#)] [[PubMed](#)]

Sample Availability: Sample of the mangiferin is available from the authors.



© 2018 by the authors. Licensee MDPI, Basel, Switzerland. This article is an open access article distributed under the terms and conditions of the Creative Commons Attribution (CC BY) license (<http://creativecommons.org/licenses/by/4.0/>).